

Impact of Phase-shift Modulation on the Performance of a Single-stage Bidirectional Electric Vehicle Charger

Diogo Varajão, Rui Esteves Araújo, Carlos Moreira and João Peças Lopes
INESC TEC, Faculty of Engineering, University of Porto, 4200-465 Porto, PORTUGAL
diogo.varajao@fe.up.pt, raraujo@fe.up.pt, cmoreira@inescporto.pt, jpl@fe.up.pt

Abstract- The Smart Vehicle-to-Grid Project at INESC TEC is currently studying the application of matrix converters to implement an isolated bidirectional AC-DC power converter using a single power conversion stage to provide a high-frequency link between the grid and vehicle. The single-stage structure and bidirectional power flow make the matrix converter an attractive solution for the charging applications of electric vehicles. A very brief overview of the matrix converter and its modulation strategy is presented, followed by detailed analysis. The power conversion system performance is investigated in terms of the switching commutation, input filter and input power factor. Simulations and experimental results of a prototype are also presented to further validate the proposed topology and operating principle.

I. INTRODUCTION

Electric vehicles (EVs) are currently emerging in the market for individual mobility and are viewed as a promising option for road transport that contributes to the reduction of greenhouse gases, increased energy conversion efficiency and reduced vehicle maintenance costs. The recent trend in the research on Smart Grids is strongly oriented to accommodate all generation devices and storage options, where the concept Vehicle-to-Grid (V2G) emerges for the EVs as a necessary technology for future power networks.

The V2G concept consists of feeding power to the grid [1] taking advantage of this vehicle's energy storage capacity [2], which can be used for peak shaving, reduced transport power losses and increased electric vehicle's integration into electric power system [3],[4]. Other ancillary services like voltage and frequency regulation and spinning reserves can also be provided to improve reliability and quality of the electric power supply [5].

These considerations bring about the requirement for a smart charger device that is capable of bidirectional power flow and communicating with energy distributors. Several topologies were analyzed in order to establish a proper on-board V2G power electronics interface for EVs. In [6] is presented an extended review of AC-DC and DC-DC converters that can be combined to form a bidirectional charger. Most of them lead to a large solution due to multiple stage conversion, and also lack isolation, such the topologies presented in [7], [8].

Solid state transformers (SST) need isolation and bidirectional power flow; then some stages of conversion can

be used to obtain a proper topology for V2G interface. Combination of AC-DC and DC-DC converters presented in [9], [10] are a possibility despite the result of a large solution. The bidirectional charger proposed in [11] is an example of this implementation with unity power factor operation capability. More compact topologies with isolation are based on dual active half bridge (DAHB) [12] and dual active bridge (DAB) [13], but both have as disadvantages the need of several capacitors and the low-power levels accepted.

Utilization of matrix converters can lead to a more simple and compact power circuit [14], since this does not need any large energy storage element and allows single-stage power conversion. In [15], [16] is proposed the utilization of two single-phase matrix converters (SPMC) in a DAB configuration in order to reduce the size of SST.

Taking this idea into account and knowing the output stage of V2G interface is to be connected to a battery pack, an SPMC at AC side and a full bridge at DC side, connected by high-frequency transformer in DAB configuration can be used. A three-phase version of this topology is presented in [17] and an improved modulation is proposed in [18], which has several advantages like single-stage power conversion, high power density, isolation, bidirectional power flow and zero current switching (ZCS) for SPMC. This modulation strategy and topology are suitable to implement the isolated bidirectional AC-DC power converter for V2G interface. The purpose of this paper is to analyze the effects of modulation on the performance of the charger.

Section II presents the proposed topology for the bidirectional charger, a brief overview of single-phase matrix converter and the mathematical model of the complete power converter system. Section III presents the methodology followed in this work. Section IV presents the simulation results obtained for modulation and for the implementation of advanced current commutation strategy. Section V presents the performance analysis of the converter and the particular issues that characterize this solution. Section VI presents experimental results that show the SPMC commutation with four-step strategy and the ZCS obtained with phase-shift modulation for this bidirectional charger topology. The conclusions are drawn in Section VII.

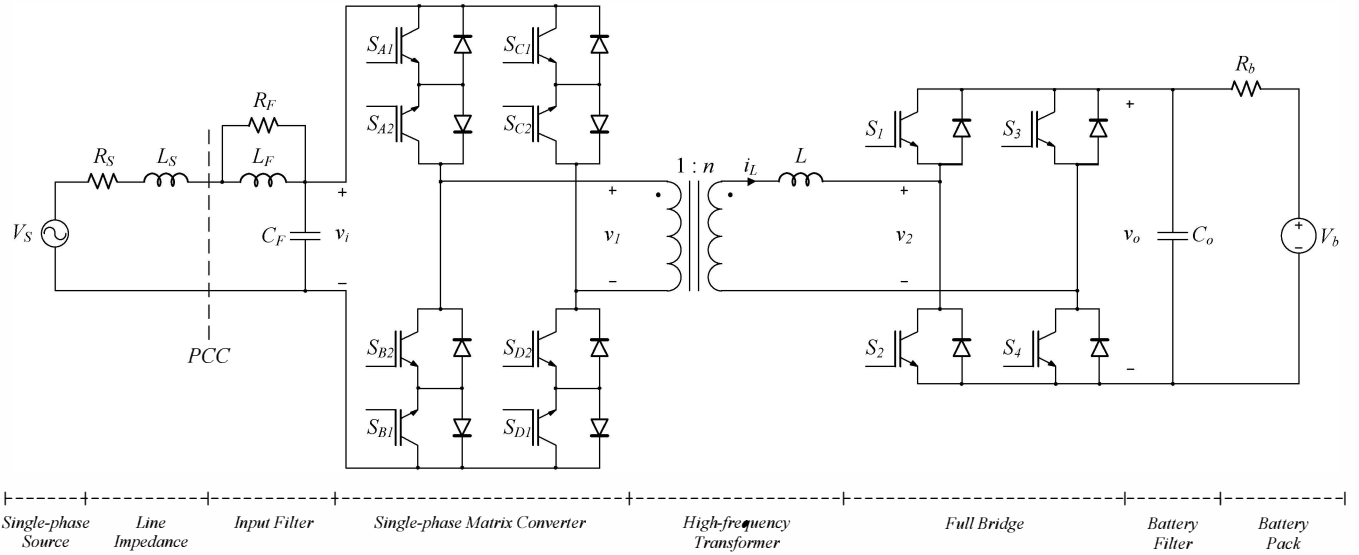


Fig. 1. Proposed single-stage bidirectional vehicle charger based on AC-DC Dual Active Bridge.

II. AC-DC DUAL ACTIVE BRIDGE IN BIDIRECTIONAL DC CHARGERS

A. Proposed Single-stage Power Converter

The proposed converter topology is shown in Fig. 1. It has two full bridges, one at the front end of the grid and the other connected to the batteries. The full bridge at the grid side is a single-phase matrix converter. The high-frequency transformer provides both galvanic isolation and energy storage through winding leakage inductance. The supply voltage at 50 Hz is converted to high-frequency switched voltages by a matrix converter. The full bridge at the battery side is the current bidirectional converter. The proposed topology can naturally allow bidirectional power flow and uses the principle of power flow in a dual active bridge converter [19]. It is well known from the theory that the active power can be controlled by 1) the phase shift between two bridges; 2) the duty ratios of switching devices; and 3) the switching frequency.

B. Matrix Converter Fundamentals and Modelling

Before going further, we should review the main features of the matrix converter in general terms. The matrix converter is a direct conversion topology in a single stage that carries out the AC-AC frequency conversion and variable voltage. The left side of Fig. 1 depicts the topology of the matrix converter of 2×2 switch cells. Each of the four switch cells is composed of common emitter back-to-back IGBTs, which allow current to flow in both directions, as well as bidirectional voltage blocking and providing controlled bidirectional power flow.

The operation of the matrix converter can be expressed mathematically in a matrix formulation, $s(t)$, using the concept of switching function [20]. The notion of commutation cell is assumed in this concept, where the switching function, s_{kj} , is defined as the representation of the switch connecting input line k to output line j . When the

switch is ON, the switching function has a value of 1, and when the switch is off, the switching function has a value of 0. Consequently, the commutation cell needs only one switching function, $s(t)$, to represent its state at any moment. The instantaneous current and voltage relationships can then be written as given in (1) and (2):

$$v_o(t) = s(t) v_i(t) \quad (1)$$

$$i_i(t) = s^T(t) i_o(t) \quad (2)$$

where $v_i(t)$ and $v_o(t)$ are the input and output voltage, s^T is the transpose matrix of s , $i_i(t)$ and $i_o(t)$ are input and output current of the commutation cell.

Before formulating the mathematical model, the following assumptions are given:

- 1) The converter is operated in steady state,
- 2) all the switches are ideal with anti-parallel diodes,
- 3) the dynamic of the input filter and magnetizing current of the transformer are negligible, and
- 4) L contains all the leakage inductance of the transformer.

Taking these assumptions into account, v_i in Fig. 1 is a pure sine wave, at the fundamental input frequency, f_i . We shall derive a converter model on the assumption that the switching frequency, f_s , is fixed and fixed duty-cycle, d , during a period of commutation. In such a case, the voltage at the transformer input side is given by

$$v_1(\tau) = s_1(\tau) v_i(\tau) \quad (3)$$

where the switching function at single-phase matrix converter, $s_1(\tau)$, is

$$s_1(\tau) = \begin{cases} 1 & 0 \leq \tau < \frac{1}{2} T_s \\ -1 & \frac{1}{2} T_s \leq \tau \leq T_s \end{cases} \quad (4)$$

where τ is used to denote the time within a commutation period and $T_s=1/f_s$.

Using the same procedure as before, the voltage at the transformer output side may be written as

$$v_2(\tau) = s_2(\tau)v_o(\tau) \quad (5)$$

and the switching function at full bridge, $s_2(\tau)$, is

$$s_2(\tau) = \begin{cases} 0 & 0 \leq \tau < \frac{1}{4} T_s (1 + \delta - d) \\ \text{sgn}(v_i) & \frac{1}{4} T_s (1 + \delta - d) \leq \tau \leq \frac{1}{4} T_s (1 + \delta + d) \\ 0 & \frac{1}{4} T_s (1 + \delta + d) < \tau < \frac{1}{4} T_s (3 + \delta - d) \\ -\text{sgn}(v_i) & \frac{1}{4} T_s (3 + \delta - d) \leq \tau \leq \frac{1}{4} T_s (3 + \delta + d) \\ 0 & \frac{1}{4} T_s (3 + \delta + d) < \tau \leq T_s \end{cases} \quad (6)$$

The phase-shift, δ , can vary between -1 and 1 and is restricted according (7) with duty-cycle, d , defined by (8).

$$|\delta| \leq 1 - d \quad (7)$$

$$d = \frac{|v_i|n}{v_o} \quad (8)$$

Assume that i_L and v_o are state variables, then the model of the power converter can be written as

$$\frac{di_L(\tau)}{d\tau} = \frac{s_1(\tau)}{L}nv_i(\tau) - \frac{s_2(\tau)}{L}v_o(\tau) \quad (9)$$

$$\frac{dv_o(\tau)}{d\tau} = -\frac{1}{R_bC_o}v_o(\tau) + \frac{V_b}{R_bC_o} + \frac{s_2(\tau)}{C_o}i_L(\tau). \quad (10)$$

III. REAL ANALYSIS METHODOLOGY

The method of real analysis used in this work consists of three steps. It is based on a mathematical model of the complete power converter system. Such an approach requires different simulation tools and more computer time; but, it offers more accurate results, the possibility of harmonic analysis, and also the impact on performance of the power converter.

The first step is modeling the complete bidirectional converter topology with the frequency AC link. The model consists of single-phase matrix converter at the front end of the grid, a full bridge interfacing the batteries, the modulation strategy and power supply model. These models are brought together, forming the complete model of the bidirectional charger.

TABLE I
SIMULATION VALUES

V_i	325V
V_b	400V
R_b	0.5 Ω
C_o	1500 μ F
f_i	50Hz
f_s	2.5kHz
n	0.3
L	100 μ H

The second step is studying the commutation problem. Particular attention must be paid to definition of the proper timing and synchronization of the switch's command signals. Authors have chosen the PSpice software, as it proved the most convenient for this purpose.

The third step is performing harmonic calculations using FFT and analysis of the power factor. The results are then represented in the form of diagrams, graphs, time traces and so on.

IV. SIMULATION RESULTS

This section presents work carried out in developing a diagram of simulation models using the Power System Blockset library within the Matlab/Simulink (MLS) environment and simulation in PSpice.

A. Bidirectional AC-DC Converter model

Computer simulation is done using ideal switches for the Matlab simulation, while PSpice was used to provide results closer to the practical implementation. The HF transformer was modeled ideally by a Linear Transformer block, except for the secondary leakage inductance which has been included. Table I gives details of the parameters used on the simulation.

B. Modulation model

Modulation is the process used to obtain the appropriate firing pulses to each switch in order to get control of the power flow. Therefore, the main objectives of this modulation

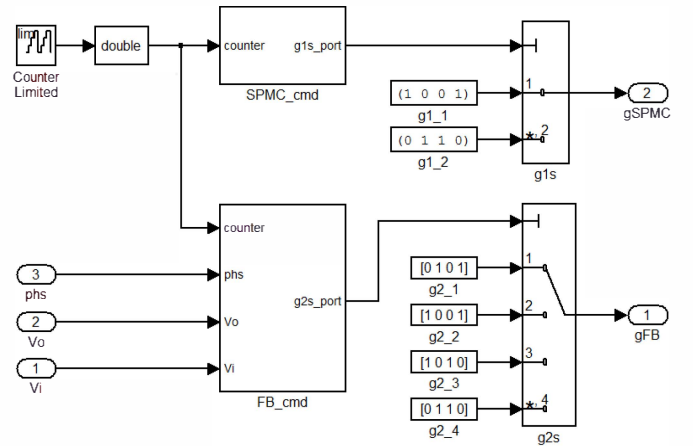


Fig. 2. Modulation model for generating gate pulses for the bidirectional AC-DC Dual Active Bridge.

are two: first is to produce a square wave with fixed frequency and variable amplitude applied to the primary of the HF transformer from the power source; second, to introduce a phase-shift angle between the outputs of both full bridges and impose that the switching of the matrix converter happen with zero current by d control. Fig. 2 presents the Simulink model for generating gate pulses for the switches. The blocks “SPMC_cmd” and “FB_cmd” determine the gate pulses for single-phase matrix converter and for full bridge, respectively. This is done based on actual period instant generated by a counter and operation parameters as phase-shift (phs in figure), V_o and V_i .

C. Power supply and filter models

Power source is represented by ideal sinusoidal single-phase source with series connection of short-circuit reactance of the power source (R_s and L_s). The source can be assumed sinusoidal, due to high short-circuit power of the supply (strong network) at the point of common coupling (PCC) [21]. The introduction of the switching-ripple-filter circuit, represented by L_F , C_F and R_F in Fig. 1, is necessary to meet international power quality standards [22]. However, this question was not analyzed in this paper and $v_i(t)$ is represented by ideal sinusoidal single-phase source.

D. Current Commutation

The modulation imposes ZCS for all the switches of the input converter in all load conditions, so in theory it is not necessary to employ an advanced commutation strategy for the switching cells, like for instance, a four-step commutation.

Fig. 3 depicts two time periods of the proposed modulation. The grid voltage is applied in HF transformer by SPMC and surge at secondary with amplitude scaled by turns ratio $1:n$. The full bridge generates v_2 with amplitude equal to battery voltage. The current i_L in leakage inductance L changes according to v_1 and v_2 . In the several simulations carried out was verified a near zero current, but in certain instants the error reached 3A. The explanation for this is probably the numerical simulation errors that led to a small slip in the full bridge commutation instants.

In a practical implementation, both grid and battery voltage measurements are subjected to noise and delays that affect

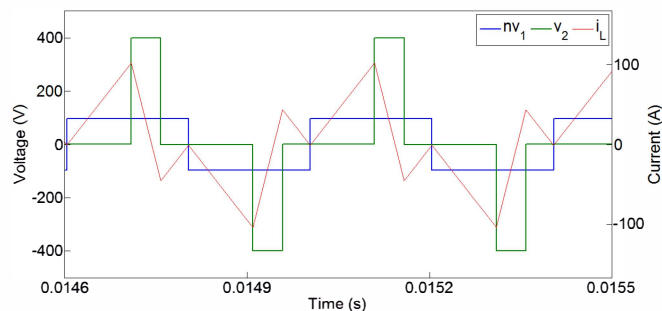


Fig. 3. Two time periods of proposed modulation.

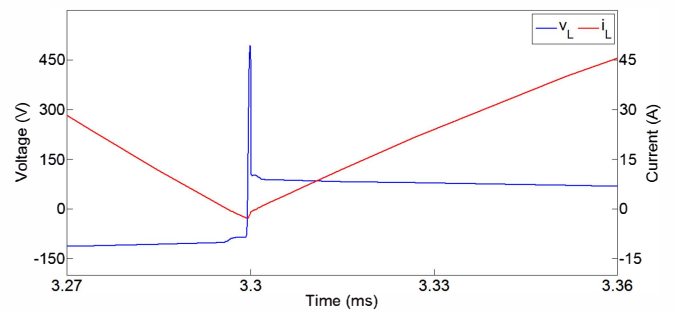


Fig. 4. Results of non-null current commutation with a dead-time.

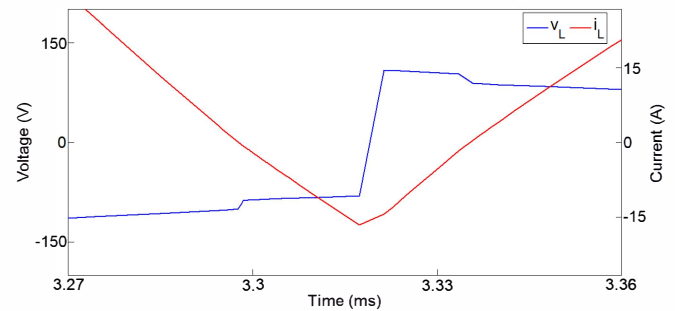


Fig. 5. Results of non-null current commutation with four-step strategy.

duty-cycle calculation and consequently the gate pulses generation, leading to a non-null current commutation and a need for an advanced commutation strategy to solve the commutation problem described in [22].

In order to study the impact of non-null current commutation, a simulation in PSpice was done of the proposed converter. The gate pulses for each commutation cell were generated with a dead-time of $1\mu s$ to prevent short-circuiting the grid side. Fig. 4 shows the voltage and current in the leakage inductance L that surges when the matrix converter switches at $-3A$. The overvoltage spike, reaching almost $500V$ due to a momentary open circuit of HF transformer, could destroy the power semiconductors. Moreover, this energy loss decreases the efficiency of power conversion and increases the size of the cooler system.

To allow the safe operation of bidirectional switches, the four-step commutation strategy was introduced in simulation [22]. Fig. 5 also shows v_L and i_L , but this time for a $-15A$ commutation. This strategy eliminated overvoltage spikes even for this current level and lowered the losses, ensuring a correct commutation despite non-null current.

V. IMPACT ON CHARGER PERFORMANCE AND HARMONIC ANALYSIS

The total harmonic distortion (THD) of SPMC input current for this operation point is near 150% (see Fig. 6), which is inappropriate for a grid interface at the PCC, because it will cause a certain level of harmonic pollution in voltage. So, as mentioned above, it is necessary to have a well-designed filter to minimize the impact on power quality in the supply network. Note that the input filter for the matrix

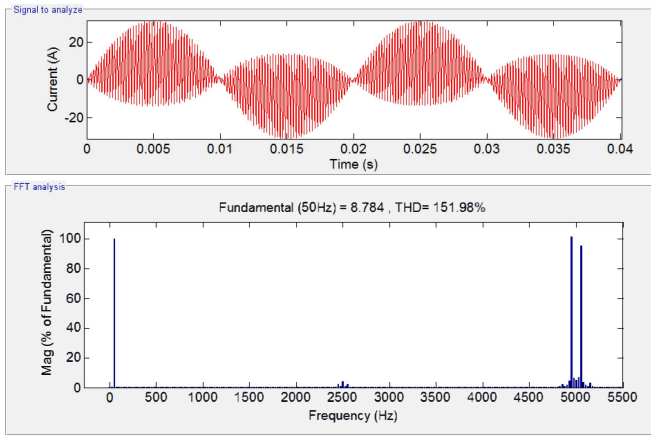


Fig. 6. Current and FFT analysis at SPMC input.

converter is a very critical element of this conversion topology in order to ensure high input power quality.

For this operation point the average power provided for the battery is around 2.0 kW, and the current peak at the secondary transformer reaches 100A. This forces the use of switches with power ratings much higher than the converter power, which constitutes a disadvantage of this modulation. Moreover, due to the large ripple verified in Fig. 6 current, the filter capacitor C_F should have a low ESR to minimize voltage fall and losses.

This modulation ensures a unitary power factor at SPMC input. The introduction of an input filter can cause a displacement in power source current related to voltage, so this should be taken into account during filter design. The impossibility of power factor control is a limitation if it is desired to change the current phase.

VI. EXPERIMENTAL RESULTS

The AC-AC stage based on SPMC was implemented with a four-step strategy in order to verify simulation results about current commutation presented in section IV. The input voltage came from an autotransformer and the SPMC output is connected to an RL load based on a 4kW rheostat box in series with a $300\mu\text{H}$ inductance. Fig. 7 presents the experimental results for one grid period with a switching frequency of 2.5 kHz. The load current commutation occurs properly and changes according SPMC output voltage. As can be seen, this commutation strategy eliminates overvoltage spikes and allows the safe operation of bidirectional switches.

After validation of SPMC operation was implemented the AC-DC DAB topology in order to validate the modulation presented in section II. As with the previous experiment, the input voltage came from an autotransformer and the SPMC is connected to the full bridge by a $300\mu\text{H}$ inductance, used to simulate all the leakage inductance of the transformer. The full bridge DC link has a $C_o=1500\mu\text{F}$ and is connected to a lead acid battery pack with 384V nominal voltage and 2.7kWh. The commutation frequency is 5 kHz and the phase-shift in this test is $\delta=0.40$. Figures 8 and 9 present the

experimental results of AC-DC DAB operation. The full bridge pulses are synchronized with SPMC output voltage,

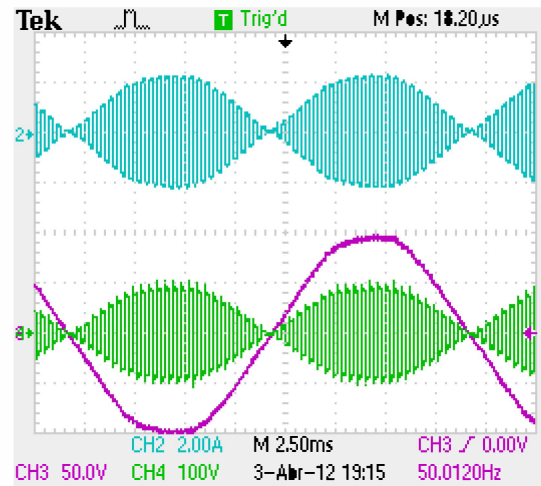


Fig. 7. Experimental results of SPMC operation with four-step strategy: output current (CH2), input voltage (CH3) and output voltage (CH4).

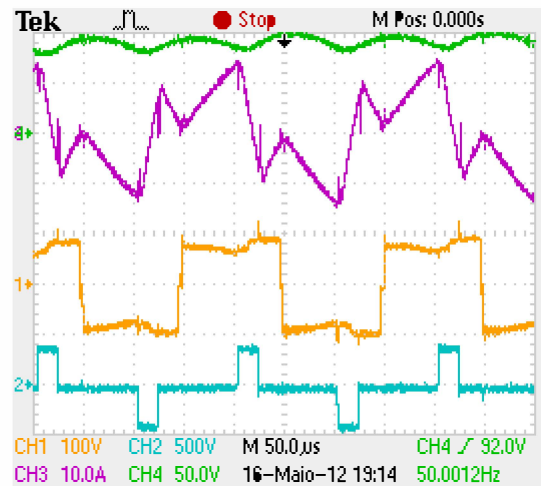


Fig. 8. Experimental results of AC-DC DAB operation with $\delta=0.40$ (period with $v_1>0$): v_1 (CH1), v_2 (CH2), i_L (CH3) and v_1 (CH4).

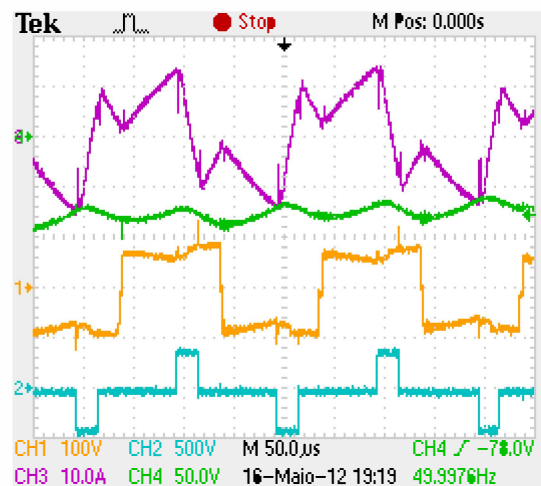


Fig. 9. Experimental results of AC-DC DAB operation with $\delta=0.40$ (period with $v_1<0$): v_1 (CH1), v_2 (CH2), i_L (CH3) and v_1 (CH4).

and also for periods with v_1 positive (Fig. 8) and negative (Fig. 9), and have a positive phase-shift for this operation point. The current in the inductance evolves with the difference between v_1 and v_2 voltages. As can be seen, the SPMC commutation occurs with near zero current (ZCS), revealing an important advantage of this modulation. These experiments allowed validation of the modulation proposed for this topology.

VII. CONCLUSION

This brief paper sheds light on some of the advantages and disadvantages of the modulation strategy proposed in [18]. The impact of phase-shift modulation for a bidirectional electric vehicle charger was analyzed. Despite the theory that this modulation imposes ZCS, our work has shown that an advanced current commutation strategy is necessary for SPMC bidirectional switches. Practical results validate the correct operation with a four-step strategy. Due to grid-side current distortion created by converter operation, a well-designed input filter is necessary to comply with power quality standards. It should be stressed that the input filter originates a displacement between grid voltage and the current that needs to be minimized during filter design. A major disadvantage of this modulation is that it cannot manipulate the phase angle of the current, and consequently imposes unity input power factor. Experimental results show the implementation of AC-DC DAB and the operation with the proposed modulation that was validated with success.

ACKNOWLEDGMENT

The authors would like to thank Miguel Miranda for their help and collaboration during the implementation of the experimental setup used in this paper.

This work is part-funded by National Funds through the FCT – Fundação para a Ciência e a Tecnologia (Portuguese Foundation for Science and Technology) within project PTDC/EEA-EEL/103546/2008 (MicroGrids+EV).

REFERENCES

- [1] S. E. Letendre and W. Kempton, "The V2G concept: A new model for power? Connecting utility infrastructure and automobiles," *Public Utilities Fortnightly*, pp. 16-26, 15 February 2002.
- [2] J. Tomić and W. Kempton, "Using fleets of electric-drive vehicles for grid support," *Journal of Power Sources*, vol. 168, pp. 459-468, 2007.
- [3] J. A. P. Lopes, F. J. Soares, and P. M. R. Almeida, "Integration of Electric Vehicles in the Electric Power System," *Proceedings of the IEEE*, vol. 99, pp. 168-183, 2011.
- [4] P. M. R. Almeida, J. A. P. Lopes, F. J. Soares, and M. H. Vasconcelos, "Automatic Generation Control operation with electric vehicles," in *Bulk Power System Dynamics and Control (iREP) - VIII (iREP)*, 2010 iREP Symposium, 2010, pp. 1-7.
- [5] W. Kempton and J. Tomić, "Vehicle-to-grid power fundamentals: Calculating capacity and net revenue," *Journal of Power Sources*, vol. 144, pp. 268-279, 2005.
- [6] D. C. Erb, O. C. Onar, and A. Khaligh, "Bi-directional charging topologies for plug-in hybrid electric vehicles," in *Applied Power Electronics Conference and Exposition (APEC)*, 2010 Twenty-Fifth Annual IEEE, 2010, pp. 2066-2072.
- [7] M. C. Kisacikoglu, B. Ozpineci, L. M. Tolbert, and F. Wang, "Single-phase inverter design for V2G reactive power compensation," in *Applied Power Electronics Conference and Exposition (APEC)*, 2011 Twenty-Sixth Annual IEEE, 2011, pp. 808-814.
- [8] S. Jaganathan and G. Wenzhong, "Battery charging power electronics converter and control for plug-in hybrid electric vehicle," in *Vehicle Power and Propulsion Conference*, 2009. VPPC '09. IEEE, 2009, pp. 440-447.
- [9] F. Haifeng and L. Hui, "High-Frequency Transformer Isolated Bidirectional DC-DC Converter Modules With High Efficiency Over Wide Load Range for 20 kVA Solid-State Transformer," *Power Electronics, IEEE Transactions on*, vol. 26, pp. 3599-3608, 2011.
- [10] S. Xu, S. Lukic, A. Q. Huang, S. Bhattacharya, and M. Baran, "Performance evaluation of solid state transformer based microgrid in FREEDM systems," in *Applied Power Electronics Conference and Exposition (APEC)*, 2011 Twenty-Sixth Annual IEEE, 2011, pp. 182-188.
- [11] R. J. Ferreira, L. M. Miranda, R. E. Araújo, and J. P. Lopes, "A New Bi-Directional Charger for Vehicle-to-Grid Integration," in *Innovative Smart Grid Technologies (ISGT)*, 2011, 2011, pp. 1-5.
- [12] N. Tuan, W. Jehyuk, and N. Kwanghee, "A single-phase bidirectional dual active half-bridge converter," in *Applied Power Electronics Conference and Exposition (APEC)*, 2012 Twenty-Seventh Annual IEEE, 2012, pp. 1127-1133.
- [13] K. E. H. Alonso, A. K. H. Harb, and L. D. P. Martinez, "Modulation characteristics for a bidirectional AC-DC converter based on dual active bridge (January 2010)," in *Electronics, Circuits and Systems (ICECS)*, 2011 18th IEEE International Conference on, 2011, pp. 293-296.
- [14] P. W. Wheeler, J. Rodriguez, J. C. Clare, L. Empringham, and A. Weinstein, "Matrix converters: a technology review," *Industrial Electronics, IEEE Transactions on*, vol. 49, pp. 276-288, 2002.
- [15] Q. Hengsi and J. W. Kimball, "Ac-ac dual active bridge converter for solid state transformer," in *Energy Conversion Congress and Exposition*, 2009. ECCE 2009. IEEE, 2009, pp. 3039-3044.
- [16] H. M. Hanafi, M. K. Hamzah, and N. R. Hamzah, "Modeling of electronic transformer design with the implementation of Single-Phase Matrix Converter using MATLAB/Simulink," in *Research and Development (SCORed)*, 2009 IEEE Student Conference on, 2009, pp. 407-410.
- [17] N. D. Weise, K. K. Mohapatra, and N. Mohan, "Universal utility interface for Plug-in Hybrid electric vehicles with vehicle-to-grid functionality," in *Power and Energy Society General Meeting*, 2010 IEEE, 2010, pp. 1-8.
- [18] N. D. Weise, K. Basu, and N. Mohan, "Advanced modulation strategy for a three-phase AC-DC dual active bridge for V2G," in *Vehicle Power and Propulsion Conference (VPPC)*, 2011 IEEE, 2011, pp. 1-6.
- [19] M. N. Kheraluwala, R. W. Gascoigne, D. M. Divan, and E. D. Baumann, "Performance characterization of a high-power dual active bridge," *Industry Applications, IEEE Transactions on*, vol. 28, pp. 1294-1301, 1992.
- [20] P. Wood, *Switching Power Converters: Van Nostrand Reinhold Company*, New York, 1981.
- [21] T. Hoevenaars, K. LeDoux, and M. Colosino, "Interpreting IEEE STD 519 and meeting its harmonic limits in VFD applications," in *Petroleum and Chemical Industry Conference*, 2003. Record of Conference Papers. IEEE Industry Applications Society 50th Annual, 2003, pp. 145-150.
- [22] P. Wheeler and D. Grant, "Optimised input filter design and low-loss switching techniques for a practical matrix converter," *Electric Power Applications, IEE Proceedings -*, vol. 144, pp. 53-60, 1997.